Journal of Industrial Microbiology, 12 (1993) 211–220

Published by The Macmillan Press Ltd

Dynamics of heat destruction of spores: a new view

G. H. Smerage and A. A. Teixeira

Department of Agricultural Engineering, University of Florida, Gainesville, FL 32611, USA

(Received 30 November 1992)

Key words: Spore survivors; Heat destruction; Population models; *Bacillus subtilis; Bacillus stearothermophilus*

SUMMARY

Discrepancies between actual, viable spore populations and those predicted by a classical model during heat sterilization of food and pharmaceutical products have long concerned food engineers and scientists as they pursue new sterilization techniques, including ultra-high temperature processes. Among potential causes of those discrepancies, activation of dormant spores is significant, and models addressing that factor were developed recently. This paper reviews historic and current views on the biology and models of microbial spore populations during heat sterilization. Activation and inactivation of viable spores are emphasized, with each viewed as a first-order reaction. Rate constants of those reactions may differ significantly, inactivation rates of dormant and activated spores may differ, and variations of all rate constants with temperature appear to be well described by Arrhenius equations. Model-based analyses show how categories of survivor response curves observed during isothermal heat treatments can arise from simultaneous activation and inactivation of spores in an overall population. Effects of different distributions of initial subpopulations, different distributions of rate constants, and 'heat shock' for homogenizing an indicator population are shown. The complexity of new, multiple process models has not increased greatly, but the potential for accurate, dynamic prediction of product safety after prescribed sterilization has. The relevant biology is understood and accounted for more thoroughly, and it is anticipated that the new models will aid design and evaluation of new and improved sterilization processes for food and pharmaceuticals.

INTRODUCTION

The classical model of a population of bacterial spores during lethal heating is based solely on inactivation of a homogeneous, initial population of activated spores and consists mathematically of a single, first-order differential equation [1,3]. It has long been known that population dynamics predicted by that model often depart significantly from those observed in isothermal laboratory experiments; the discrepancies generally have been attributed to activation early in the heating of spores that were dormant in the initial population. Margins of safety commonly used in relatively low-temperature, long-duration sterilization of food and pharmaceutical products diminish the importance of the discrepancies and the need for more complex models. Greater importance of accurate predictions in laboratory contexts led to the common use of heat shock, sublethal heating of a spore suspension for uniform activation prior to lethal treatment, to permit use of the classical model in characterizing spores and designing and validating thermal sterilization processes.

In recent years, broader ranges of product packaging and more stringent qualities expected of sterilized products have led to new requirements and processes for thermal sterilization, including ultra-high temperature processes. The pursuit of new sterilization techniques by engineers and scientists has emphasized inadequacies of the classical model and established a need for more accurate models; it has focused attention on activation of dormant spores early in a thermal sterilization process. Several researchers have reported on this matter, and of several models proposed, those by Shull et al. [13], Rodriguez et al. [9,10], and Sapru et al. [11] are most notable. However, only the Rodriguez/Sapru model needs to be considered because it encompasses the Shull and classical models.

The Rodriguez/Sapru model offers many advantages over the classical model and will be the preferred model for many applications because it represents the broader range of biological situations extant during lethal heating of spore suspensions. Consequently, it is capable of more accurate prediction of product safety after prescribed sterilization, facilitates interpretation and understanding of the relevant biology, and obviates heat shock for the traditional purpose. The Rodriguez/Sapru model and any successors to it should become valuable tools for design, evaluation, and control of new, more sophisticated sterilization processes for food and pharmaceuticals. While superior to the classical model, complexity of the Rodriguez/Sapru model is not significantly greater; application of it is relatively simple and proceeds in a manner similar to that for the classical model.

This chapter examines behavioral features of the classical, Sapru, Rodriguez, and Shull models for the purpose of justifying the proposition that the classical model be replaced by the Rodriguez/Sapru model. Application of the Rodriguez/Sapru model is discussed, including parameter determination,

Correspondence to: G.H. Smerage, Department of Agricultural Engineering, University of Florida, Gainesville, FL 32611, USA.
Mention of brand or firm names does not constitute an endorsement by the US Department of Agriculture over others of a similar nature not mentioned.

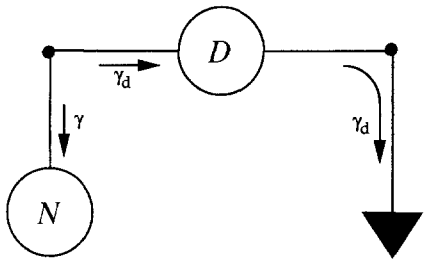

Fig. 1. Process diagram of Model 1, the classical model.

description of parameter variations with temperature by Arrhenius equations, and isothermal, dynamic, and ultra-high temperature regimes.

MODELS

A homogeneous, totally activated, single species population of bacterial spores subjected only to thermal inactivation (death) is depicted in Fig. 1. The circle labeled N represents the population; thermal inactivation, a transformation represented by the circle labeled D, transfers members from activated population N to a sink of inactivated (dead) spores depicted by the triangle. The two processes are described by:

$$N: \frac{dN}{dt} \equiv \gamma = -\gamma_d \quad D: \gamma_d \equiv K_d N \tag{1}$$

where K_d is the rate constant of the thermal death process. Combining the two descriptions yields the system equation.

$$\text{Model 1:} \quad \frac{dN}{dt} = -K_d N \tag{2}$$

This is the classical model long used in thermal sterilization [1,3].

Now let the single species population be a mix of dormant and activated, but otherwise homogeneous and viable, subpopulations and allow thermal activation of the dormant spores. This more general situation is depicted in Fig. 2, where N_1 and N_2 denote, respectively, the dormant and activated subpopulations, transformation A denotes the activation process, and D denotes inactivation. The four processes are described by:

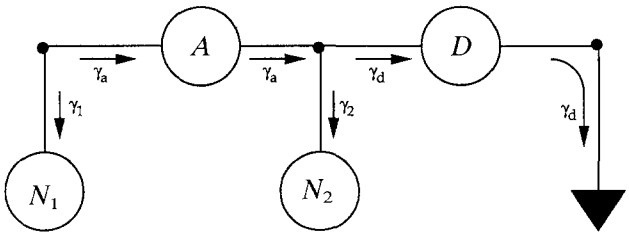

Fig. 2. Process diagram of Model 2, the Shull model.

$$N_1: \frac{d}{dt}N_1 \equiv \gamma_1 \qquad N_2: \frac{d}{dt}N_2 \equiv \gamma_2$$

$$A: \gamma_a \equiv K_a N_1 \qquad D: \gamma_d \equiv K_d N_2 \tag{3}$$

where K_a and K_d are rate constants of the processes. Structural constraints require

$$\gamma_1 \equiv -\gamma_a \quad \gamma_2 \equiv \gamma_a - \gamma_d \tag{4}$$

Appropriate combination of information in Eqns (3) and (4) yields the following mathematical model of this system.

$$\text{Model 2:} \quad \begin{aligned} \frac{d}{dt}N_1 &\equiv -K_a N_1 \\ \frac{d}{dt}N_2 &\equiv K_a N_1 - K_d N_2 \end{aligned} \tag{5}$$

This model was proposed by Shull et al. [13].

Additional generality is achieved by incorporating the possibility that lethal heating may kill some dormant spores before activating them. That possibility is included in Fig. 3, where inactivation D_1 has been added to the model in Fig. 2. With D_1 and D described by

$$D_1: \gamma_{d1} \equiv K_{d1} N_1 \quad D: \gamma_d \equiv K_d N_2 \tag{6}$$

and A described as in Eqn (3), the mathematical model can be formulated as

$$\text{Model 3:} \quad \begin{aligned} \frac{d}{dt}N_1 &\equiv -(K_a + K_{d1})N_1 \\ \frac{d}{dt}N_2 &\equiv K_a N_1 - K_d N_2 \end{aligned} \tag{7}$$

This model was proposed by Rodriguez et al. [9] with rate constant $K_{d1} = K_d$ and by Sapru et al. [11] with distinct K_{d1} and K_d.

From the above, particularly Model 3 and concepts upon which it is based, additional models can be hypothesized for even more complex situations in the biology of bacterial spores during lethal heating. That is illustrated here by just one model applicable to a complex of two types of spores having distinct thermal properties as well as dormant and activated subpopulations. Possible situations include two species or two strains of a single species differing in the sensitivities of their thermal activation and inactivation

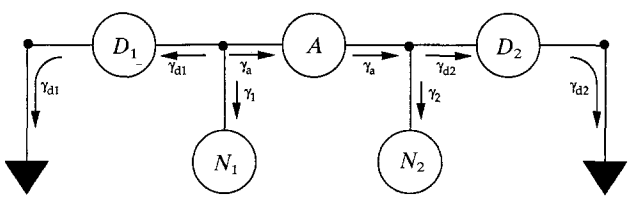

Fig. 3. Process diagram of Model 3, the Rodriguez/Sapru model.

processes, as reflected in the values of rate constants. Rodriguez et al. [9] examined this case for injured and normal subdivisions of a single species. The situation is depicted in Fig. 4 as a double replication of Fig. 3; N_{ij} denotes a subpopulation, with i indicating dormant ($i = 1$) or activated ($i = 2$) and j indicating a major subdivision ($j = 1$ or 2) of the total population. Corresponding notation applies to the rate constants: K_{aj}, K_{dj}, and K_{d1j}. Note in Fig. 4 that the major subdivisions are not connected by any process; they function independently. That property is reflected in the mathematical model below, which consists of two independent sets of two coupled differential equations. Using process descriptions similar to Eqns (3) and (6), the mathematical model for Fig. 4 is a double replication of Eqn (7) in the form:

$$\frac{d}{dt}N_{11} \equiv -(K_{a1} + K_{d11})N_{11}$$

$$\frac{d}{dt}N_{21} \equiv K_{a1}N_{11} - K_{d1}N_{21}$$

Model 4: (8)

$$\frac{d}{dt}N_{12} \equiv -(K_{a2} + K_{d12})N_{12}$$

$$\frac{d}{dt}N_{22} \equiv K_{a2}N_{12} - K_{d2}N_{22}$$

Although Models 2–4 are increasingly more complex than classical Model 1, they remain relatively simple relative to the range of population models. Yet, the incorporation of a few additional processes significantly expands behavioral features beyond those possessed by the classical model and more accurately represents bacterial spore populations for conditions extant in laboratory suspensions and food and pharmaceutical products during thermal sterilization. We now examine behavioral features of the four models, with emphasis on Model 3, since it encompasses Models 1 and 2 and is the basis for Model 4.

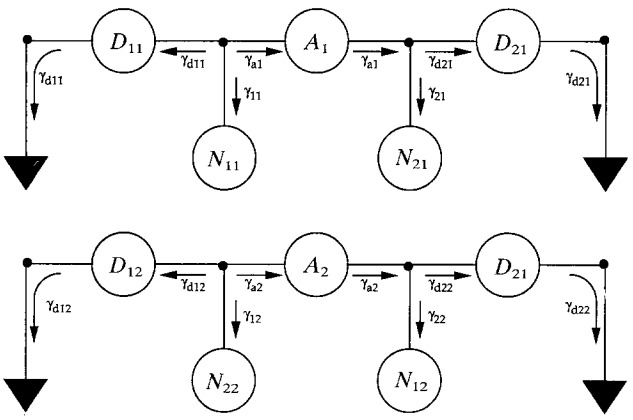

Fig. 4. Process diagram of Model 4, for two distinct subdivisions of a total spore population.

Isothermal responses

With respect to the models presented above, relevant thermal properties of bacterial spores are their rate constants of activation and inactivation and the temperature dependencies of those parameters. This information may be determined from isothermal survivor curves obtained at several temperatures. Many behavioral features of models and, in turn, real spore populations may be determined and interpreted from analyses of isothermal responses. The importance of isothermal analyses arises from the invariance of rate constants throughout isothermal heating; consequently, in such circumstances, all models presented above are linear, time invariant, and amenable to analytical solution. Furthermore, many sterilization processes are viewed ideally as isothermal.

During exposure of spores to isothermal, lethal heating, survivors are defined at instant t to be the activated spores, $N_{2j}(t)$, in each (species, strain, or other) subdivision of the total population. Only activated spores are capable of forming colonies in supportive conditions and, therefore, can be identified by standard enumeration procedures. Although potentially viable, the same is not true of dormant subpopulations, and, by convention, they are not considered survivors.

Enumeration procedures may not distinguish subpopulations, N_{2j}, in a spore complex, so care must be exercised in using and interpreting enumerated survivors. With respect to the models above, the degree of sterilization achieved at instant t by a thermal process and the potential for spoilage of product later and conveyed by the undifferentiated numbers of survivor spores, $N(t)$, and viable, dormant spores, $N_1(t)$,

$$N(t) \equiv \sum_{\forall j} N_{2j}(t) \tag{9}$$

$$N_1(t) \equiv \sum_{\forall j} N_{1j}(t) \tag{10}$$

remaining relative to their initial numbers, $N(0)$ and $N_1(0)$.

The comparative analysis of spore population models presented below utilizes the following scenario. Exposure of spores to constant temperature T occurs over time interval $(0, t_s)$. Prior to exposure, the total number of spore bodies (undifferentiated) equals DMC, the direct microscopic count. The DMC consists of dormant and activated viable subpopulations N_{ij} with initial numbers $N_{ij}(0) \equiv N_{ij0}$. The DMC may also include a subpopulation of dead spores. The initial numbers of survivors, $N(0) \equiv N_0$, and viable, dormant spores, $N_1(0) \equiv N_{10}$, are given by

$$N_0 \equiv \sum_{\forall j} N_{2j0} \tag{11}$$

and

$$N_{10} \equiv \sum_{\forall j} N_{1j0} \tag{12}$$

Consider, first, classical Model 1 containing only activated population N and described by Eqn (2). By analytical solution, only one mode of survivor curve is possible—exponential decay from initial population N_0.

$$N(t) = N_0\, e^{-K_d t} = N_0\, e^{-t/(2.3D)} \tag{13}$$

The final form of Eqn (13) invokes decimal reduction time D commonly used in thermal process calculations [16]. The semilogarithmic graph of Eqn (13), a line with slope $-K_d$ and intercept $\ln(N_0)$, generally is used to estimate N_0 and K_d or D. Reduction of N from N_0 by L log cycles requires exposure for 2.303 L K_d units of time^{-1}.

Model 2 has dormant and activated subpopulations with initial numbers N_{10} and N_{20}, respectively. Analytical solution of Eqn (5) yields survivor response N,

$$N(t) \equiv N_2(t) = N_{20}\, e^{-K_d t} + \frac{K_a}{K_a - K_d} N_{10} \left(1 - e^{-(K_a - K_d)t}\right) e^{-K_d t} \tag{14}$$

for $K_a \neq K_d$. The solution for $K_a = K_d$, available in Shull et al. [13], is not important here. The shape of this survivor curve depends on relative sizes of N_{10} and N_{20} and of K_a and K_d, and it is clear that the possibilities are much more robust than the classical response of Eqn (13). In particular, the second term in Eqn (14) can cause the shoulder often observed early in real, laboratory exposures.

The survivor response of Model 3, found by analytical solution of Eqn (7), is

$$N(t) \equiv N_2(t) = N_{20}\, e^{-K_d t} + \frac{K_a}{K_a + K_{d1} - K_d} N_{10} \left(1 - e^{-(K_a + K_{d1} - K_d)t}\right) e^{-K_d t} \tag{15}$$

Equations (14) and (15) differ little in substance, but they may differ significantly in shape for common K_a and significant difference in K_{d1} and K_d.

Finally, survivor responses for Model 4 are N_{21} and N_{22} for the individual divisions and $N = N_{21} + N_{22}$ for the whole complex, with N_{21} and N_{22} having forms like Eqn (15). With initial populations N_{110} and N_{210} for the first division and N_{120} and N_{220} for the second, analytical solution of Eqn (8) for N_{21} and N_{22} and summation of them yield survivor response

$$\begin{aligned} N(t) &= N_{21}(t) + N_{22}(t) \\ &= N_{210}\, e^{-K_{d1} t} \\ &\quad + \frac{K_{a1}}{K_{a1} + K_{d11} - K_{d1}} N_{110} \left(1 - e^{-(K_{a1} + K_{d11} - K_{d1})t}\right) e^{-K_{d1} t} \\ &\quad + N_{220}\, e^{-K_{d2} t} \\ &\quad + \frac{K_{a2}}{K_{a2} + K_{d12} - K_{d2}} N_{120} \left(1 - e^{-(K_{a2} + K_{d12} - K_{d2})t}\right) e^{-K_{d2} t} \end{aligned} \tag{16}$$

Clearly, this behavior is far beyond the simple exponential of the classical model.

Comparison of the models continues by examining graphs of their survivor responses. The analysis is facilitated by normalizing time by $1/K_d$ and N_2 by N_{20}. This choice of normalization factors was guided by the fact that K_d and N_{20} pertain to the relatively slow decay of the activated spore population, which is the focus of the classical model. With $N'_2 \equiv N_2/N_{20}$ and $t' \equiv K_d t$, survivor responses of Eqns (13), (14), and (15) become, respectively,

$$N'(t') = e^{-t'} \tag{17}$$

$$N'(t') \equiv N'_2(t') = e^{-t'} + \frac{K_a/K_d}{K_a/K_d - 1} \left[\frac{N_{10}}{N_{20}}\right] \left(1 - e^{-(K_a/K_d - 1)t'}\right) e^{-t'} \tag{18}$$

$$\begin{aligned} N'(t') &\equiv N'_2(t') \\ &= e^{-t'} + \frac{K_a/K_d}{K_a/K_d + K_{d1}/K_d - 1} \left[\frac{N_{10}}{N_{20}}\right] \left(1 - e^{-(K_a/K_d + K_{d1}/K_d - 1)t'}\right) e^{-t'} \end{aligned} \tag{19}$$

The survivor curves of Eqns (17), (18) and (19) are plotted in Fig. 5 for $N_{10}/N_{20} = 5$, $K_a/K_d = 5$, and $K_{d1} = K_d$. Although all three models begin with the same activated population, N_{20}, the curves of Eqns (18) and (19) differ considerably from the classical curve of Eqn (17) because heating activates a large portion of initially dormant spores, N_{10}, before subsequently killing most of them. Note that mortality of dormant spores before activation can significantly shift curve of Eqn (19) for Model 3 below curve of Eqn (18) for Model 2, which omits that mortality. Other choices of parameters and initial conditions cause relative shapes of the three curves to change only in degree, not substance. Of course, $N_{10} = 0$ results in Eqns (18) and (19) being identical to the simple, classical Eqn (17). Mixed suspensions of dormant/activated spores prior to lethal heat treatment are realistic situations that led to the practice of using heat shock (low temperature heating of suspension to assure uniform activation of viable spores) to permit continued use

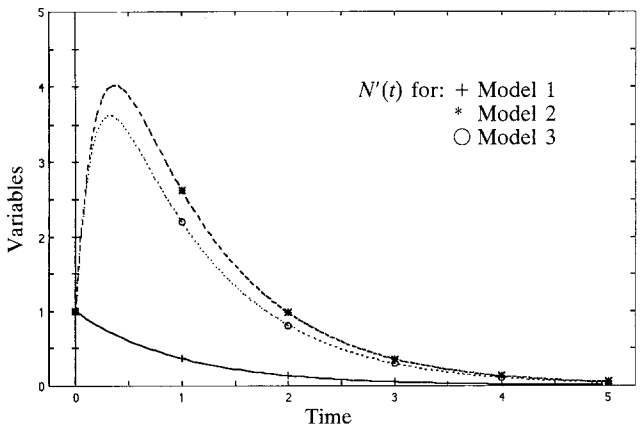

Fig. 5. Normalized, isothermal survivor curves of Models 1, 2, and 3 for $N_{10}/N_{20} = 5$ and $K_a/K_d = K_a/K_{d1} = 5$.

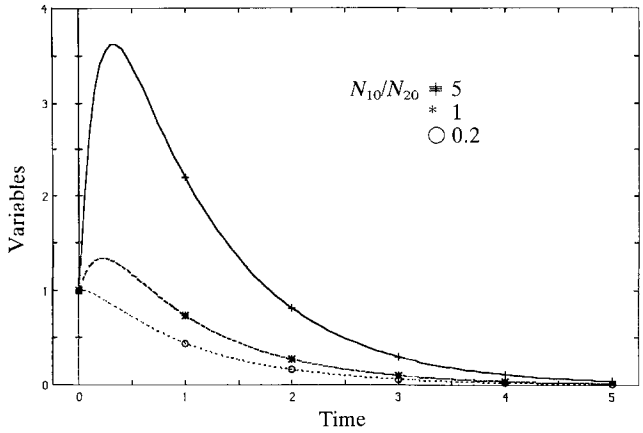

Fig. 6. Normalized survivor curves possible with Model 3 when maintaining $K_a/K_d = K_a/K_{d1} = 5$ and varying N_{10}/N_{20}.

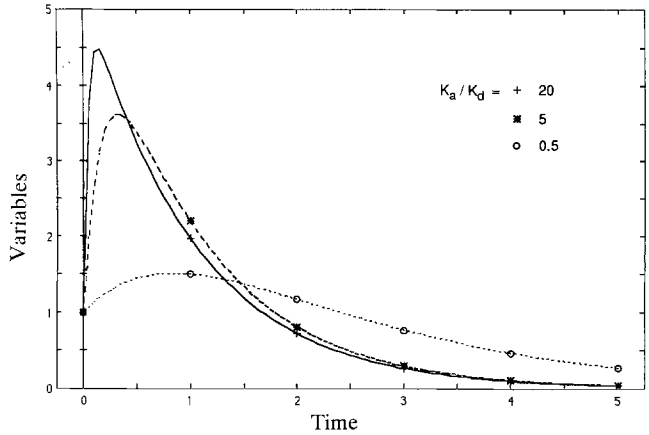

Fig. 8. Normalized survivor curves possible with Model 3 when maintaining $N_{10}/N_{20} = 5$ and $K_a/K_{d1} = 5$ while varying K_a/K_d and, thereby, K_{d1}/K_d.

of the classical model of sterilization. Use of Model 3 obviates heat shock for that purpose and permits representation of a broader range of situations.

The range of shapes of survivor curves possible with Model 3 is indicated by Figs 6, 7, and 8. In Fig. 6, $K_a/K_d = 5$ and $K_{d1} = K_d$ are maintained while N_{10}/N_{20} is varied. In Fig. 7, $N_{10}/N_{20} = 5$ and $K_a/K_d = 5$ are maintained while K_a/K_{d1} and, thereby, K_{d1}/K_d are varied. Finally, the effect of varying K_a/K_d while maintaining $N_{10}/N_{20} = 5$ and $K_a/K_{d1} = 5$ is illustrated in Fig. 8. Figures 5–8 indicate the following: activation of initially dormant spores can greatly influence the shape of a survivor curve; that influence typically occurs early in the heating; survivor curves for mixed dormant/activated initial populations are not single, simple exponentials, as has been verified frequently by experimental data; activation of initially dormant spores can cause a 'shoulder' in a survivor curve that has also been observed frequently in experimental data; the magnitude of a shoulder depends on N_{10}/N_{20} and ratios of rate constants; and classical Model 1 is inadequate for general representation of bacterial spore populations during sterilization of laboratory suspensions and food and pharmaceutical products.

Examination of Eqn (15) provides additional insight on the behavior of Model 3. The first term in Eqn (15) pertains only to inactivation of initial, activated population N_{20}; it is identical to the classical response of Eqn (13) for an initial, uniformly activated population equal to N_{20}. The second term in Eqn (15) pertains only to activation and subsequent inactivation of initial, dormant population N_{10}. Those two components add to give total survivor curve N. Normalized graphs of the components and survivor curve in Eqn (15), as given by Eqn (19) with $N' \equiv N/N_{20}$ and $t' \equiv K_d t$, are shown in Fig. 9 to illustrate the relationships. While the first term continually declines exponentially from 1 (corresponding to N_{20} in Eqn (15)) with rate constant K_d, the second term initially rises from zero due to activation of surviving members of N_{10} and peaks before declining exponentially with rate constant K_d. Depending on relative amplitudes of the two terms, reflecting N_{10}/N_{20}, K_a/K_{d1}, and K_{d1}/K_d, the second term in Eqn (19) may cause N' to rise from 1, peak, and then decline exponentially with rate constant K_d as in Fig. 9. Possible variations of N' with values of N_{10}/N_{20}, K_a/K_{d1}, and K_a/K_d were illustrated in Figs 5–8.

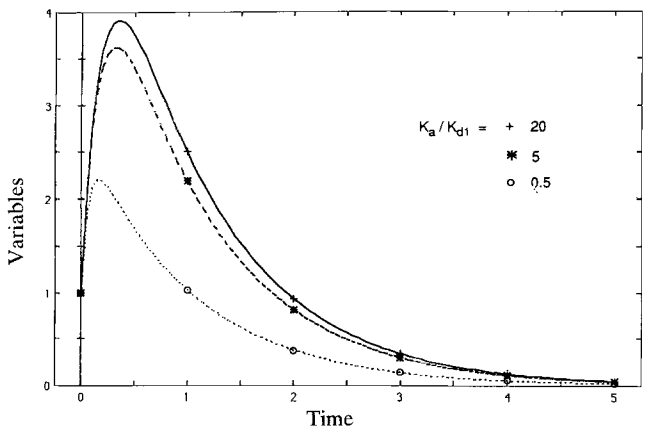

Fig. 7. Normalized survivor curves possible with Model 3 when maintaining $N_{10}/N_{20} = 5$ and $K_a/K_d = 5$ while varying K_a/K_{d1} and, thereby, K_{d1}/K_d.

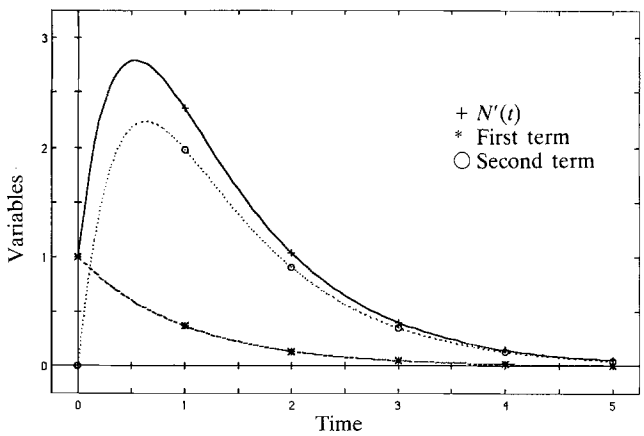

Fig. 9. Normalized graphs of first and second components in Eqn (18) add to give normalized survivor curve N′ of Model 3.

The peak value of N for Model 3 and the time, t_p, at which it occurs are found by differentiating Eqn (15), setting $dN/dt = 0$, and solving for t_p. The result is

$$t_p = \frac{1}{K_a + K_{d1} - K_d} \ln\left[\frac{\frac{K_a + K_{d1}}{K_d}}{1 + \frac{K_a + K_{d1} - K_d}{K_a}\frac{N_{20}}{N_{10}}}\right] \tag{20}$$

Using this value of t in Eqn (15), the peak value is

$$N(t_p) = N_{20}\, e^{-K_d t_p} + \frac{K_a}{K_a + K_{d1} - K_d} N_{10} \left(1 - e^{-(K_a + K_{d1} - K_d)t_p}\right) e^{-K_p t_p} \tag{21}$$

If the duration of isothermal, lethal heating exceeds $5/(K_a + K_{d1})$, the maximum possible number of initially dormant spores, $(K_a/(K_a + K_{d1}))N_{10}$, are activated early in the exposure. If the duration exceeds $5/(K_1 + K_{d1} - K_d)$, the nested exponential, $\exp(-(K_a + K_{d1} - K_d)t)$, in the second term of Eqn (15) becomes essentially zero, and, from then on, N follows

$$N(t) \approx \left[N_{20} + \frac{K_a}{K_a + K_{d1} - K_d} N_{10}\right] e^{-K_d t} \tag{22}$$

which is the tail of the survivor curve due to predominant inactivation. In this region, the curve is an exponential that appears to have begun with pseudo initial activated population $N_{20} + (K_a/(K_a + K_{d1} - K_d))N_{10}$.

Figure 10 demonstrates the high quality of predictions by Model 3 through comparison at four lethal temperatures of model predicted isothermal survivor curves, (Eqn (15)), with data from corresponding experiments for *Bacillus stearothermophilus* spores. Similar comparisons for other species of spores and for numerous replications have proven equally well [9,10,11].

The diversity of responses of Model 4 for two types of spores is great, and only two situations are examined here. Normalizing time by $1/K_{d2}$ and N by N_{220}, parameters of activated spores of the second type, $t' \equiv t/K_{d2}$ and Eqn (16) becomes

$$\begin{aligned} N'(t') &\equiv \frac{1}{N_{220}} N(t') = \frac{1}{N_{220}} N_{21}(t') + \frac{1}{N_{220}} N_{22}(t') \equiv N'_{21}(t') + N'_{22}(t') \\ &= \frac{N_{210}}{N_{220}} e^{-K_{d1}/K_{d2} t'} + \frac{K_{a1}/K_{d1}}{K_{a1}/K_{d1} + K_{d1}/K_{d1} - 1}\left[\frac{N_{110}}{N_{220}}\right] \\ &\quad \left[1 - \exp\left[-\left[\frac{K_{a1}}{K_{d2}} + \frac{K_{d11}}{K_{d2}} - \frac{K_{d1}}{K_{d2}}\right]t'\right]\right] e^{-K_{d1}/K_{d2} t'} \\ &\quad + e^{-t'} + \frac{K_{a2}/K_{d2}}{K_{a2}/K_{d2} + K_{d12}/K_{d2} - 1}\left[\frac{N_{120}}{N_{220}}\right] \\ &\quad \left[1 - \exp\left[-\left[\frac{K_{a2}}{K_{d2}} + \frac{K_{d12}}{K_{d2}} - 1\right]t'\right]\right] e^{-t'} \end{aligned} \tag{23}$$

In the first case considered, both types of spores are initially present in equal proportions, type 1 spores are moderately more sensitive to heat than type 2 spores, and activation of both types is more rapid than inactivation: $N_{210}/N_{220} = 1$, $N_{110}/N_{210} = N_{120}/N_{220} = 5$; $K_{d1}/K_{d2} = 2$, $K_{a1}/K_{d1} = K_{a1}/K_{d11} = 10$, $K_{a2}/K_{d2} = 2$, $K_{a2}/K_{d12} = 5$. For those conditions, Fig. 11 shows normalized survivor curves N'_1 for type 1, N'_2 for type 2, and $N' = N'_1 + N'_2$ for all spores. The second case is similar to the first except that type 1 spores are much more sensitive to heat than type 2 spores, and the two types are not initially present in equal proportions: $N_{210}/N_{220} = 2$, $N_{110}/N_{210} = 5$, $N_{120}/N_{220} = 10$; $K_{d1}/K_{d2} = 20$, $K_{a1}/K_{d1} = K_{a1}/K_{d11} = 10$, $K_{a2}/K_{d2} = 0.5$, $K_{a2}/K_{d12} = 5$. Figure 12 shows normalized component and aggregate survivor curves for those conditions. Responses in Fig. 11 are compatible with those in Figs 5–8 and introduce nothing new. Figure 12 introduces another mode of aggregate survivor curve that has been observed experimentally [9, 16]. It exhibits a very fast initial increase and subsequent, slightly slower decline due primarily to very rapid activation and inactivation of type 1 spores. The curve continues with a slower increase, attributable to activation of initially dormant type 2 spores, followed by an even slower decline caused by inactivation of activated, type 2 spores. With the

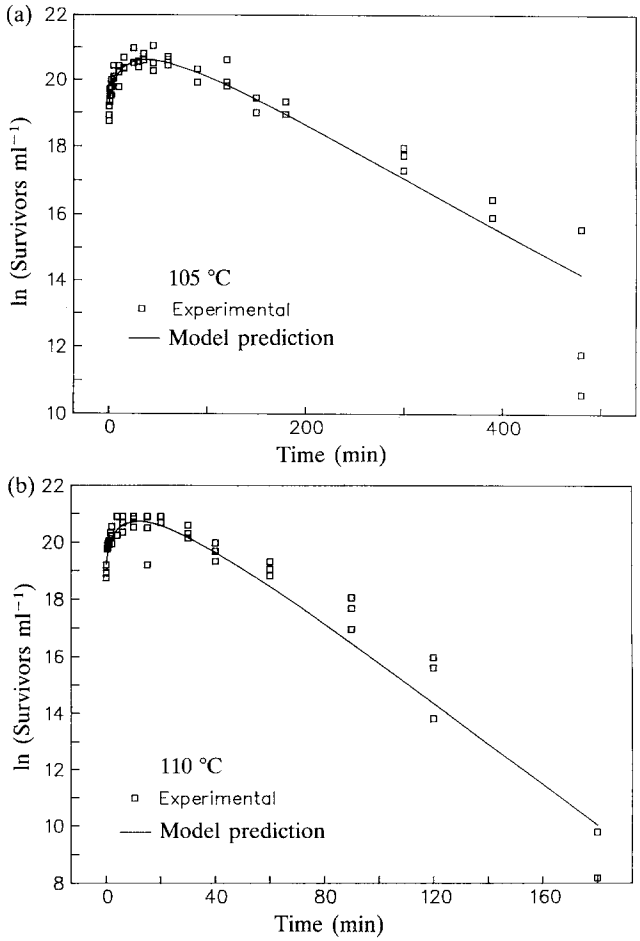

Fig. 10. (a)–(d). Predicted and corresponding experimental, isothermal survivor curves of *B. stearothermophilus* spores at 105, 110, 115, and 120 °C demonstrate the high quality of predictions by Model 3 [11].

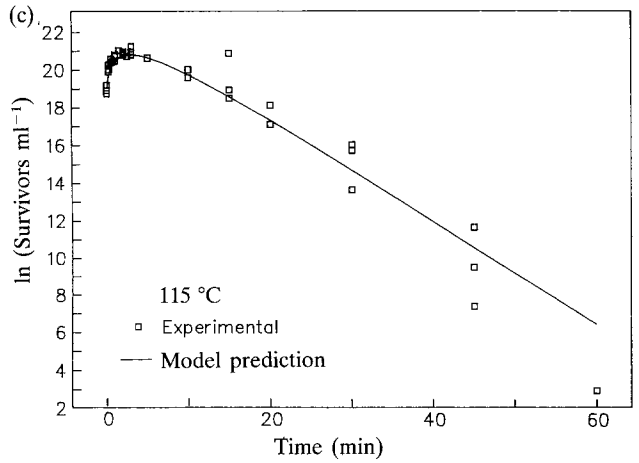

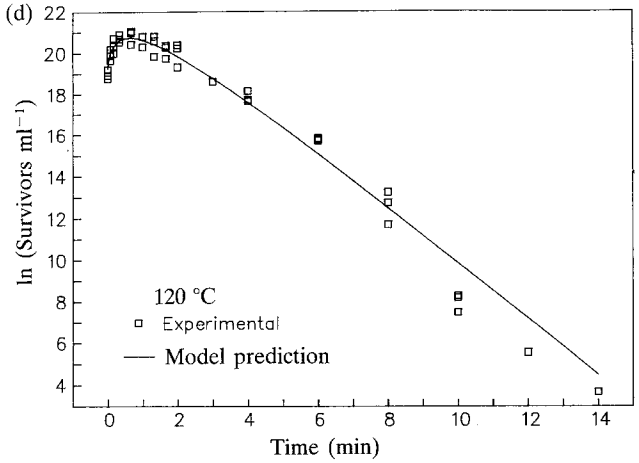

Fig. 10. (c) & (d).

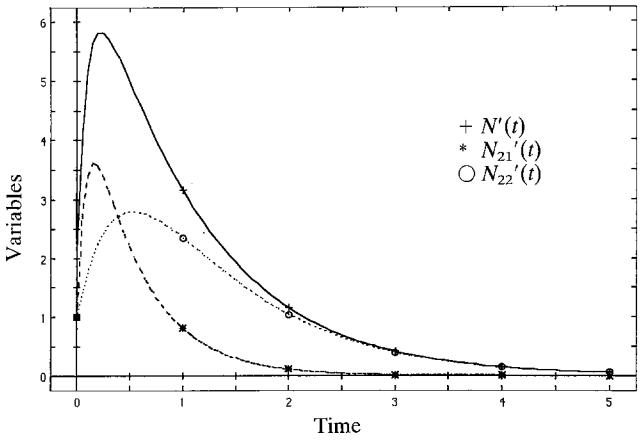

Fig. 11. Normalized survivor curves N'_{21} and N'_{22} of type 1 and type 2 spores in Model 4 and aggregate curve $N' = N'_{21} + N'_{22}$ when the two types initially are equally present with type 1 spores moderately more sensitive to heat than type 2 and activation of both more rapid than inactivation. The conditions: $N_{210}/N_{220} = 1$, $N_{110}/N_{210} = N_{120}/N_{220} = 5$; $K_{d1}/K_{d2} = 2$, $K_{a1}/K_{d1} = K_{a1}/K_{d11} = 10$, $K_{a2}/K_{d2} = 2$, $K_{a2}/K_{d12} = 5$.

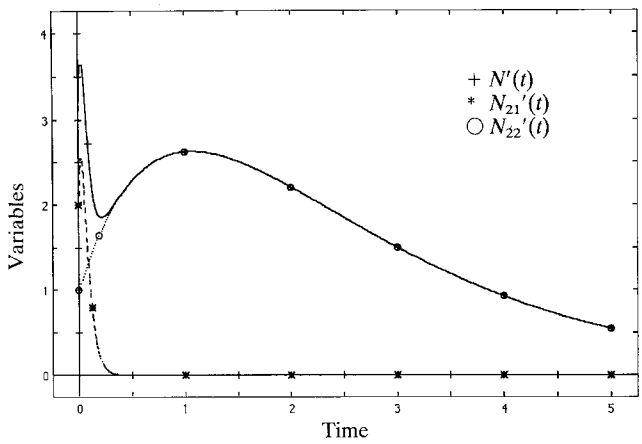

Fig. 12. Normalized survivor curves N'_{21} and N'_{22} of type 1 and type 2 spores in Model 4 and aggregate curve $N' = N'_{21} + N'_{22}$ when the two types initially are present in different proportions with type 1 spores much more sensitive to heat than type 2 and activation of both more rapid than inactivation. The conditions: $N_{210}/N_{220} = 2$, $N_{110}/N_{210} = 5$, $N_{120}/N_{220} = 10$; $K_{d1}/K_{d2} = 20$, $K_{a1}/K_{d1} = K_{a1}/K_{d11} = 10$, $K_{a2}/K_{d2} = 0.5$, $K_{a2}/K_{d12} = 5$.

much faster rate constants of type 1 spores, all the action is over for type 1 spores before activation of type 2 is finished.

Activation and heat shock

It has been common practice to heat suspensions of spores at sublethal, constant temperature prior to using them in experiments for thermal characterization of spores and validation of sterilization processes. The purpose has been to activate dormant spores initially present and achieve a uniformly activated suspension appropriate to representation during lethal heating by classical Model 1 given in Eqn (2). Empirical requirements for the procedure exist [2,4,5,7,14,15], but Model 3 provides another basis for the requirements.

The first part of Eqn (7) describes the fate of a single type of initially dormant spore, N_{10}, in a suspension during both sublethal and lethal heating; its isothermal response,

$$N_1(t) = N_{10}\, e^{-(K_a + K_{d1})t} \tag{24}$$

permits calculation of the time required at specified temperature to activate a suspension uniformly. Reduction of dormant subpopulation N_1 from initial value N_{10} to negligible value N_{1f} can be expressed in terms of $L \equiv \log (N_{10}/N_{1f})$. At the specified sublethal temperature, K_a and K_{d1} have specific values, and the time, t_{hs}, required to reduce N_1 by L log cycles is readily found from Eqn (24) to be:

$$t_{hs} = 2.3\, \frac{L}{(K_a + K_{d1})} \tag{25}$$

Therefore, to reduce the initial, dormant subpopulation of a suspension to negligible value expressed by L log cycles

of reduction, isothermal heating at the specified sublethal temperature for t_{hs} units of time is required.

During heat shock, activated spore population $N = N_2$ changes according to Eqn (15) from initial value N_{20} to final value $N(t_{hs})$. For subsequent lethal heating of the suspension, $N_0 \equiv N(t_{hs})$ is the appropriate initial condition for representing N by classical Eqn (2). With t_{hs} sufficiently long, the parenthesis in the second term of Eqn (15) essentially equals 1, and

$$N_0 \equiv N(t_{hs}) \approx \left[N_{20} + \frac{K_a}{K_a + K_{d1} - K_d} N_{10}\right] e^{-K_d t_{hs}} \qquad (26)$$

Note from Eqn (26) that, in general, $N_0 \neq N_{20} + N_{10}$. Logarithmic reduction, L, and duration, t_{hs}, of heat shock must be selected to assure that $N_1 \approx 0$ and Eqn (26) hold for $t > t_{hs}$, otherwise Eqn (26) and use of the classical model will not be valid.

Dynamic and UHT responses

Dynamic responses of models are important to the design and biological validation of sophisticated, modern, sterilization systems because in many cases temperature regimes are dynamic rather than constant and rate constants are functions of temperature. It follows that rates of activation and inactivation vary throughout dynamic thermal processes and complicate predictions of spore population dynamics, especially in ultra-high temperature, short-duration (UHT) processes. This section briefly indicates the dynamic response capabilities of the Rodriguez/Sapru model, Model 3 in Eqn (7), and complements earlier discussion of its isothermal responses.

Isothermal responses N_1 and $N = N_2$ of Model 3 given by Eqns (24) and (15), respectively, are not valid in dynamic, lethal temperature regimes because K_a, K_d, and K_{d1} vary with temperature and it is not mathematically proper merely to vary each rate constant in Eqns (24) and (15) with temperature. For each dynamic, lethal heating, Eqn (7) must be solved by analytical means or computer simulation over the interval of heating while varying all rate constants in response to temperature variation and incorporating initial populations N_{10} and N_{20}. Temporal variation of each rate constant over a heating interval is accomplished by operating on the temperature regime with the static function relating each rate constant to temperature. Those functions must be known over the range of temperature to be investigated; they are determined by experiments mentioned briefly in the next section.

The next few figures demonstrate the performance capabilities of Model 3 for dynamic, lethal temperature regimes. Figure 13(a) presents survivor curves of *B. subtilis* spores simulated by Model 3 and Model 1, the latter for two extremes of initial, activated population N_0, in response to the dynamic temperature in Fig. 13(b) [10]. The curves demonstrate earlier discussion about responses of the two models differing significantly early in lethal heating due to activation of a significant initial, dormant population in Model 3. Note that tails of the curves are similar in shape

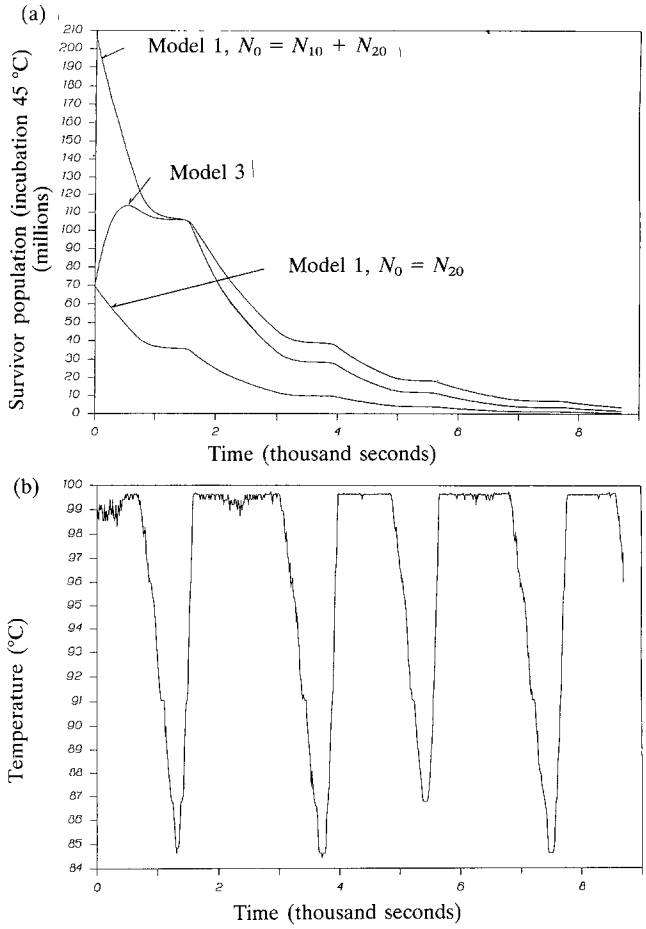

Fig. 13. Survivor curves (a) of *B. subtilis* spores simulated by Model 3 and Model 1, the latter for two extremes of initial, activated population N_0, in response to the dynamic temperature in (b) [10].

because only inactivation of activated spores occurs in that region but are offset because initial conditions of the three curves differ substantially. Note further the dynamic correspondences between input temperature and responses—plateaux in survivor curves correspond to large, negative excursions of temperature and large declines in populations occur during high temperature. Figure 14 demonstrates how well experimental survivor curves of *B. stearothermophilus* spores compare with those simulated with Model 3 for a dynamic temperature also shown in the figure [11].

In a series of ultra-high temperature (UHT) experiments, suspensions of *B. stearothermophilus* spores were subjected to 123–146 °C peak value and 6–73 s duration rectangular pulses of temperature [11]. It was not possible to measure survivor curves at points spread over the heating intervals, so just numbers of survivors at the conclusion of UHT treatments were measured and compared with values predicted by simulations with Model 3. The simulation used actual UHTs as input and initial dormant and activated populations as initial conditions. The scatter diagram in Fig. 15 comparing predicted and measured values is generally favorable. High numbers of survivors resulted for lower temperature short duration UHT treatments, where the dynamics correspond to early stages of isothermal survivor curves when both activation and inactivation function

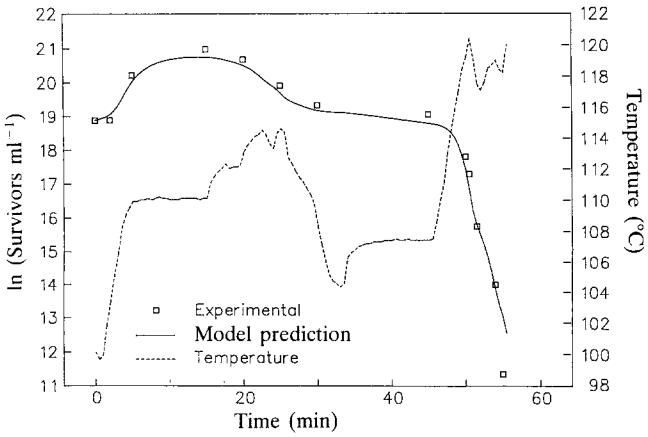

Fig. 14. Experimental survivor curve of *B. stearothermophilus* spores and corresponding curve simulated with Model 3 for the dynamic temperature shown [11].

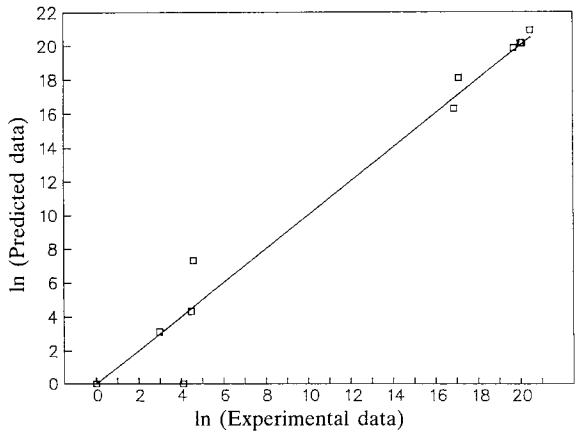

Fig. 15. Scatter diagram of numbers of *B. stearothermophilus* survivors at the conclusion of UHT treatments measured in the laboratory and predicted by Model 3 [11].

strongly. Low numbers of survivors resulted for higher temperature and longer duration because full traversal of the survivor curve and high reduction of the initial, viable population was accomplished.

Application of the Rodriguez/Sapru model

Advantages of the Rodriguez/Sapru model make it preferable to the classical model for many applications; this section provides an overview of its application. First, suitability of the model for representing a specific situation is assessed by ascertaining that it involves heating of a homogeneous, single species/strain population of spores in potentially mixed dormant/activated states. If a different, or more complex situation exists, a new model should be developed consistent with the concepts and methods embodied in the Rodriguez/Sapru model. Such was exemplified by Model 4 in this paper and a model of a combined population of normal and injured spores by Rodriguez et al. [9]. In the sequel, the Rodriguez/Sapru model is assumed to be suitable to the situation addressed.

Quantitative application of the Rodriguez/Sapru model requires species/strain specific values of rate constants K_a, K_d, and K_{d1} and initial subpopulations N_{10} and N_{20}, respectively, of dormant and activated spores. Initial subpopulations in a sample of untreated suspension or product are determined under the common assumption that all spores in a direct microscopic count (DMC) of the sample are viable [6]. Incubation of the sample and enumeration of colony-forming units yields the initial number of activated spores, N_{20}, and the initial number of dormant spores, N_{10}, is calculated from

$$N_{10} = \mathrm{DMC} - N_{20} \tag{27}$$

Rate constants for a specific species/strain of spores at specified temperature are obtained by analysis of an experimental, isothermal survivor curve for a suspension of those spores and known values of N_{10} and N_{20}. Specifically, K_a, K_{d1}, and K_{d2} are estimated by nonlinear regression, with the procedure in SAS [11,12] or by Levenburg–Marquardt [8, 9,10] fitting Eqn (15) of the model to data defining the experimental curve. Initial estimates of K_a, K_{d1}, and K_d required by the nonlinear procedures are appropriately calculated from the data by the method of successive residuals [10].

Rate constants estimated at a single temperature apply only to that temperature. Applications of the model for other constant or dynamic temperature regimes require estimates of the rate constants and, preferably, continuous functions describing them as functions of temperature over a range of temperature. It follows that isothermal experiments and estimations of rate constants must be performed at several temperatures over the prescribed range, and expressions relating rate constants to temperature must be found by regressing graphs of rate constants vs temperature. This was done for *B. subtilis* spores over 87–99 °C by Rodriguez et al. [10] and for *B. stearothermophilus* spores over 105–120 °C by Sapru et al. [11]. In both cases, dependencies of rate constants of activation and inactivation on temperature were described well by the empirical Arrhenius equation [17],

$$K = A\, e^{-E_a/RT} \tag{28}$$

where K denotes a rate constant, A = frequency constant (time^{-1}), E_a = activation energy (J mol^{-1}), T = absolute temperature (°K), and R = gas constant (8.314 J mol^{-1} °K^{-1}). Estimation of A and E_a is usually done by regressing semilogarithmic plots of rate constant date and Eqn (28); i.e. Arrhenius plots of ln K vs $1/T$ from Eqn (28).

$$\ln(K) = \ln(A) - \frac{E_a}{R}\frac{1}{T} \tag{29}$$

Use of the Rodriguez/Sapru model at UHT is contingent upon the ability to determine valid rate constants in that range, but generation of isothermal, UHT survivor curves

for parameter estimation is difficult. An approach to the matter is extrapolation to UHT of results obtained at lower lethal temperatures, using the Arrhenius equations established for that range. In a series of UHT experiments with *B. stearothermophilus* spores over 123–146 °C by Sapru et al. [11], rate constants in that range estimated with Arrhenius equations established at 105–120 °C gave very good agreement between model predicted (by simulation) and experimental numbers of survivors at the conclusion of UHT heating.

With rate constants and their dependencies on temperature for a specific species/strain of spores known and with N_{10} and N_{20} known for dormant and activated subpopulations of those spores in a specific suspension or product, the dynamics of those subpopulations and the survivor curve caused by specific, lethal heating of the suspension or product may be estimated by computer simulation or analytical solution of the Rodriguez/Sapru model given by Eqn (7). Both simulation and analytical solution of Eqn (7) are readily accomplished on a microcomputer, and graphs of the temperature regime and response variables, e.g. N_1 and $N = N_2$, over the exposure interval are the most useful forms of output. During a simulation or analytical solution, rate constants are varied as temperature varies by means of the Arrhenius equations; those variations of rate constants are the only way temperature enters the model and affects population dynamics. Temperature may be constant or dynamic and in the low or UHT lethal range. Such analyses of the behavior of the model enable one to predict, understand, and interpret the dynamics and effectiveness of existing and proposed sterilization processes, and the Rodriguez/Sapru model should be a tool in the design and validation of new, thermal sterilization processes.

CONCLUSION

The classical model of bacterial spore populations during thermal sterilization inadequately represents biological situations commonly extant in spore suspensions and food and pharmaceutical products. The Rodriguez/Sapru model offers many advantages and will be preferred for many applications because it represents the broader range of situations extant during lethal heating of spore populations. Parameters of the Rodriguez/Sapru model for a specific species/strain of spores are readily determined by isothermal experiments. Dependencies of the parameters on temperature in the lower, lethal range, e.g. 100–120 °C, are well described by Arrhenius equations that may be used to estimate values of the parameters for UHT. The Rodriguez/Sapru model obviates heat shock commonly employed to permit use of the classical model.

With rate constants of the Rodriguez/Sapru model and their dependencies on temperature known for a specific, single species/strain of spores and with initial dormant and activated subpopulations of those spores known for a specific, unsterilized suspension or product, the dynamics of those subpopulations in response to a specific thermal sterilization process and the effectiveness of the process may be estimated by computerized analyses of the model. The temperature may be constant or dynamic and in the low or UHT lethal range. The Rodriguez/Sapru model is useful for analysis, understanding, and interpretation of existing and proposed sterilization processes and in the design and validation of new processes.

REFERENCES

1 Ball, C.O. and F.C.W. Olson. 1957. Sterilization in Food Technology, Ch. 4, pp. 157–179. McGraw-Hill Book Co., New York.

2 Busta, F.F. and Z. John Ordal. 1963. Heat-activation kinetics of endospores of *Bacillus subtilis*. Food Sci. 29: 345.

3 Chick, H. 1910. The process of disinfection by chemical agencies and hot water. J. Hygiene 10: 237–286.

4 David, J.R.D. and R.L. Merson. 1990. Kinetic parameters for inactivation of *Bacillus stearothermophilus* at high temperatures. J. Food Sci. 55(2): 488.

5 Davies, F.L., H.M. Underwood, A.G. Perkin and H. Burton. 1977. Thermal death kinetics of *Bacillus stearothermophilus* spores at ultra high temperatures. I. Laboratory determination of temperature coefficients. J. Food Technol. 12: 115.

6 Gombas, D.E. 1987. Bacterial sporulation and germination. In: Topics in Food Microbiology. Vol I, Concepts in Physiology and Metabolism (Montville, T.J., ed.), Ch. 5, pp. 141–146, CRC Press, Boca Raton, FL.

7 Kimsey, H.R., D.M. Adams and J.J. Kabara. 1981. Increased inactivation of bacterial spores at high temperatures in the presence of monoglycerides. J. Food Safety, 3: 69.

8 Press, W.H., B.P. Flannery, S.A. Teukolsky and W.T. Vetterling. 1986. Numerical Recipes: The Art of Scientific Computing, Ch. 14, pp. 523–528. Cambridge University Press, Cambridge.

9 Rodriguez, A.C., G.H. Smerage, A.A. Teixeira and F.F. Busta. 1988. Kinetic effects of lethal temperatures on population dynamics of bacterial spores. Transactions of the ASAE 31(5): 1594–1606.

10 Rodriguez, A.C., G.H. Smerage, A.A. Teixeira, J.A. Lindsay and F.F. Busta. 1992. Population model of bacterial spores for validation of dynamic thermal processes. J. Food Proc. Eng. 15: 1–30.

11 Sapru, V., A.A. Teixeira, G.H. Smerage and J.A. Lindsay. 1992. Predicting thermophilic spore population dynamics for UHT sterilization processes. J. Food Sci. 57(5): 1248–1252, 1257.

12 SAS Users Guide: Statistics. 1985. SAS Institute Inc., Cary, NC.

13 Shull, J.J., G.T. Cargo and R.R. Ernst. 1963. Kinetics of heat activation and thermal death of bacterial spores. Appl. Microbiol. 11: 485.

14 Srimani, B. and M. Loncin. 1980. Determination of Decimal Reduction Time of *Bacillus stearothermophilus* and *Bacillus subtilis* spores at 100 °C. Lebensmit-Wissenschaft Technol. 13: 190.

15 Srimani, B., R. Stahl and M. Loncin. 1980. Death rates of bacterial spores at high temperatures. Lebensmit-Wissenschaft Technol. 13: 186.

16 Stumbo, C.R. 1965. Thermobacteriology in Food Processing, Ch. 7, pp. 70–86. Academic Press, New York.

17 Williams, V.R. and H.B. Williams. 1973. Basic Physical Chemistry for the Life Sciences, 2nd end, Ch. 6, pp. 313–320. W.H. Freeman and Co., San Francisco.